Current Biology 24, 1383–1389, June 16, 2014 ©2014 Elsevier Ltd All rights reserved http://dx.doi.org/10.1016/j.cub.2014.05.005

Report

Protein Delivery to Vacuole Requires SAND Protein-Dependent Rab GTPase Conversion for MVB-Vacuole Fusion

Manoj K. Singh,[1] Falco Krüger,[2] Hauke Beckmann,[1] Sabine Brumm,[1] Joop E.M. Vermeer,[3,5] Teun Munnik,[3] Ulrike Mayer,[4] York-Dieter Stierhof,[4] Christopher Grefen,[1] Karin Schumacher,[2] and Gerd Jürgens[1,*]

[1]Center for Plant Molecular Biology (ZMBP), Developmental Genetics, University of Tübingen, Auf der Morgenstelle 32, 72076 Tübingen, Germany

[2]Center for Organismal Studies (COS), University of Heidelberg, 69120 Heidelberg, Germany

[3]Section Plant Physiology, University of Amsterdam, Swammerdam Institute for Life Sciences, 1098 SM, Amsterdam, the Netherlands

[4]Center for Plant Molecular Biology (ZMBP), Microscopy, University of Tübingen, 72076 Tübingen, Germany

Summary

Plasma-membrane proteins such as ligand-binding receptor kinases, ion channels, or nutrient transporters are turned over by targeting to a lytic compartment—lysosome or vacuole—for degradation. After their internalization, these proteins arrive at an early endosome, which then matures into a late endosome with intraluminal vesicles (multivesicular body, MVB) before fusing with the lysosome/vacuole in animals or yeast [1, 2]. The endosomal maturation step involves a SAND family protein mediating Rab5-to-Rab7 GTPase conversion [3]. Vacuolar trafficking is much less well understood in plants [4–6]. Here we analyze the role of the single-copy *SAND* gene of *Arabidopsis*. In contrast to its animal or yeast counterpart, *Arabidopsis* SAND protein is not required for early-to-late endosomal maturation, although its role in mediating Rab5-to-Rab7 conversion is conserved. Instead, *Arabidopsis* SAND protein is essential for the subsequent fusion of MVBs with the vacuole. The inability of *sand* mutant to mediate MVB-vacuole fusion is not caused by the continued Rab5 activity but rather reflects the failure to activate Rab7. In conclusion, regarding the endosomal passage of cargo proteins for degradation, a major difference between plants and nonplant organisms might result from the relative timing of endosomal maturation and SAND-dependent Rab GTPase conversion as a prerequisite for the fusion of late endosomes/MVBs with the lysosome/vacuole.

Results and Discussion

Endocytosis is crucial in controlling the plasma-membrane protein repertoire in all eukaryotic cells. Membrane proteins such as cell-surface receptors are delivered to the lumen of the lytic compartment (lysosome or vacuole) for degradation. On their way, proteins endocytosed from the plasma membrane successively pass through the early endosome (EE) and the late endosome (LE) before reaching the lytic compartment (vacuole/lysosome). Recent evidence suggests that early endosomes mature into late endosomes containing intraluminal vesicles—so-called multivesicular bodies (MVBs)—through a process of Rab GTPase conversion [7]. This process involves Mon1/SAND protein, which together with CCZ1 acts as a guanine-nucleotide exchange factor (GEF) on Rab7-type GTPases that also inactivates Rab5-type GTPases [1, 3, 8, 9].

The lack of an independent early endosome (EE) is a distinguishing feature of the plant endomembrane system [10, 11]. In plants, the trans-Golgi network (TGN) is the first compartment reached by endocytic cargo and is thus at the crossroads of the secretory and endocytic routes [12]. Importantly, Rab5-like GTPases as well as phosphatidylinositol-3-phosphate (PI3P), hallmarks of yeast and animal early endosomes, are largely absent from the plant TGN/EE [13, 14]. Nevertheless, it has recently been proposed that MVBs mature from the TGN/EE [15] and we have thus investigated whether the single-copy *Arabidopsis SAND* gene is involved in TGN/EE-to-MVB maturation and/or whether it plays a role in mediating Rab5-to-Rab7 conversion.

Endosomal maturation from TGN/EE to MVB was examined in *Arabidopsis* seedling root cells, via pairwise colabeling of three marker proteins: TGN/EE-localized subunit a1 of V-ATPase (VHA-a1) [10], Rab5-like GTPase ARA7 (aka RABF2b) [13], and the fluorescent PI3P sensor YFP-2xFYVE [14]. In line with previous findings, colocalization between VHA-a1 and ARA7 was generally low as ARA7 mostly accumulated at the MVB [10, 16]. However, ARA7 also marked a subdomain of the VHA-a1-positive TGN/EE (Figure 1A). The dual localization of ARA7 to TGN/EE and MVB has also been observed in EM images of immunolabeled cryosections [13]. In contrast, 2xFYVE was separate from, but often abutted, the TGN/EE (Figure 1B). ARA7 was mostly colocalized with 2xFYVE, which labeled an additional subpopulation of endosomes devoid of ARA7 (Figure 1C). Upon BFA treatment, which causes aggregation of TGN/EEs into "BFA compartments" that do not include MVBs [16], some ARA7 colocalized with VHA-a1 in BFA compartments although the majority of the ARA7 signal still gave a distinct punctate pattern (Figure 1D). In contrast, the 2xFYVE signal was not altered such that the BFA compartments were exclusively ARA7 positive in double-labeled root cells (Figure 1E). Taken together, these results suggest that endosomal maturation in *Arabidopsis* appears to originate in a subdomain of the TGN/EE that recruits Rab5-like ARA7 and subsequently matures into an MVB, and this transition is accompanied by the accumulation of PI3P (Figure 1F). This conclusion is supported by ultrastructural studies indicating MVB formation on Golgi-associated tubular-vesicular structures, the local presence of ESCRT proteins on TGN/EE, and the strong reduction in the number of MVBs observed after inhibition of the V-ATPase in the TGN/EE [15].

The *Arabidopsis* genome harbors a single-copy *SAND* gene encoding a member of the eukaryotic SAND/Mon1 protein family and this gene appears to be expressed at moderate level throughout development (Figures S1A and S1B available online). Two mutant alleles, *sand-1* and *sand-2*, caused by T-DNA insertional gene inactivation (Figures S1C and S1D), impaired seed germination, seedling root growth, and plant growth but had almost no adverse effect on gametophyte

[5]Present address: Department of Plant Molecular Biology (DBMV), University of Lausanne, UNIL-Sorge, 1015 Lausanne, Switzerland

*Correspondence: gerd.juergens@zmbp.uni-tuebingen.de

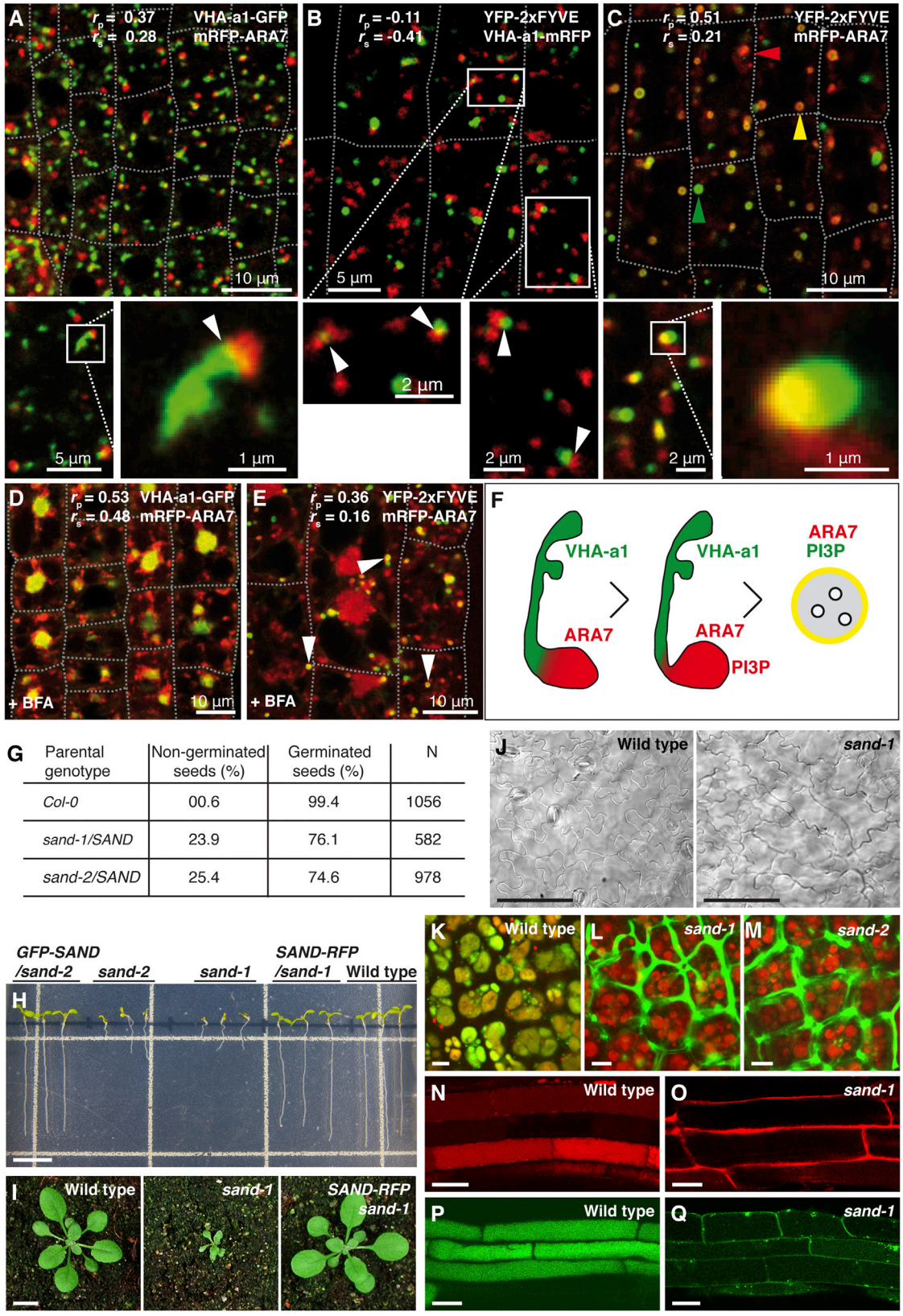

Figure 1. Spatial Relationship of TGN and MVB Markers, *sand* Mutant Phenotype, and Membrane Trafficking Defects

(A) Localization of VHA-a1-GFP and mRFP-ARA7. The lower panels show both proteins at a higher magnification, revealing a subdomain of mRFP-ARA7 at the VHA-a1-GFP-labeled TGN. Fluorescence in lower panel was recorded with a pinhole diameter of 0.37 AU.

(B) Localization of YFP-2xFYVE and VHA-a1-mRFP. The lower panels show corresponding close-up views where small areas of overlap are visible. The images were obtained with a pinhole diameter of 0.37 AU.

(legend continued on next page)

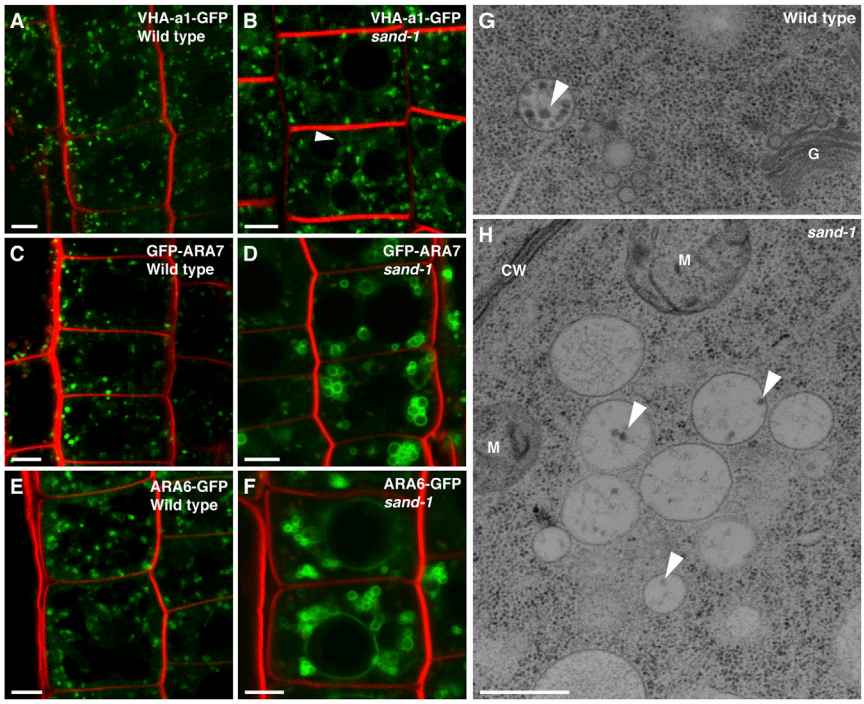

Figure 2. SAND Protein Acts at MVBs

(A and B) Localization of TGN-resident VHA-a1-GFP in wild-type and *sand-1*. Note additional faint labeling of vacuolar membrane in *sand-1* (B; arrowheads).

(C and D) ARA7-positive organelles are enlarged and clustered in *sand-1* (D).

(E and F) ARA6-positive organelles are enlarged and clustered in *sand-1* (F). In addition, ARA6 labeling of vacuolar membrane is also observed (F).

(G and H) Electron micrographs of clusters of enlarged MVBs in *sand-1* (H) as compared to wild-type (G). Note the presence of intraluminal vesicles in MVB clusters in *sand-1* similar to wild-type (arrowheads). CW, cell wall; G, Golgi stack; M, mitochondrion.

Scale bars represent 5 μm (A–F); 500 nm (G, H). See also Figure S2.

development or function (Figures 1G–1I and S1E–S1J). In addition, the pavement cells of the cotyledon epidermis were much less lobed in *sand-1* than in wild-type (Figure 1J). Similarly, cell sizes and cell shapes in the seedling root appeared abnormal (Figure S1G). These defects were abolished by expression of N-terminally GFP-tagged SAND driven by *UBQ10* promoter or C-terminally mRFP-tagged SAND under the control of *RPS5A* promoter, indicating that SAND protein is required in all those developmental contexts (Figures 1H, 1I, and S1).

To identify the trafficking pathway(s) in which SAND acts, we analyzed the subcellular localization of pathway-specific markers (Figures 1K–1Q and S2). Vacuolar marker proteins comprised fluorescent protein fusions of sorting signals from two storage proteins, α′-subunit of β-conglycinin (CT24) [17] and phaseolin (AFVY) [15], and the soluble protease aleurain fused to GFP [18], normally being delivered to the protein storage vacuole or the lytic vacuole, respectively. Rather than being delivered to the vacuole, all three soluble marker proteins for vacuolar trafficking were secreted from the cell (Figures 1K–1Q). These trafficking defects impair storage protein accumulation and vacuolar protein breakdown, limiting nutrients for growth, and might thus explain the developmental defects described above (see Figures 1K–1Q). In contrast, there was no detectable effect on secretory or recycling post-Golgi trafficking pathways. Cytokinesis-specific syntaxin KNOLLE [19] accumulated at the cell plate as in wild-type (Figures S2A and S2B), auxin efflux carrier PIN1 [20] was localized at the basal plasma membrane (Figures S2C and S2D), and PIN2 [21] accumulated at the apical end of epidermal cells (Figures S2E and S2F). The steady-state accumulation of the two PIN proteins at the plasma membrane results from their continuous cycling through endosomes [20, 21]. However, some aberrant endosomal localization of PIN2, but not PIN1, was detected (Figures S2E and S2F), which might suggest that vacuolar trafficking of PIN2 is impaired, consistent with the higher turnover of PIN2 as compared to PIN1 [21]. Thus, late secretory and recycling traffic from the TGN to the plasma membrane or the cell division plane does not require SAND function and SAND appears to be specifically required for protein delivery to the vacuole.

To delineate the site of action of SAND protein, we analyzed the subcellular localization of TGN and MVB markers in both wild-type and *sand-1* mutant seedling roots (Figure 2).

(C) Overview of YFP-2xFYVE and mRFP-ARA7 showing independent green and red signals together with compartments of merged fluorescence, marked with color-coded arrowheads. The close-up views reveal that some of these compartments display a gradual fluorescence distribution.

(D) VHA-a1GFP and mRFP-ARA7 after BFA treatment (50 μM, 30 min).

(E) YFP-2xFYVE and mRFP-ARA7 after BFA treatment (50 μM, 30 min). Note that some ring-like signals of YFP-2xFYVE still colocalize with mRFP-ARA7 on MVB (arrowheads).

(F) Schematic diagram showing spatial relationship between VHA-a1, ARA7, and PI3P. A subdomain of a TGN undergoing maturation becomes enriched with ARA7 and subsequently with PI3-kinases, generating a membrane domain positive for both ARA7 and PI3P. Once an MVB is pinched off from the TGN, its surface is covered with both PI3P and ARA7.

(G) Germination defect in *sand* mutant seeds. Homozygous mutant progeny (25% expected) from *sand-1*/SAND and *sand-2*/*SAND* mother plants often fail to germinate.

(H) Root growth of *sand* mutant seedlings is impaired. The growth of *sand-1* and *sand-2,* complemented by transgene is similar to that of wild-type.

(I) Homozygous *sand-1* showed severe dwarf phenotype on soil. The growth defects of *sand-1* plants expressing SAND-RFP were fully rescued.

(J) Reduced lobing of epidermal pavement cells in *sand-1* cotyledons.

(K–M) Storage vacuole marker GFP-CT24 delivered to the storage vacuole (red) in developing seeds of wild-type (K) but secreted from the cell in *sand-1* (L) and *sand-2* (M).

(N–Q) Phaseolin vacuolar targeting sequence AFVY fused to RFP (N, O) and lytic-vacuole marker aleurain fused to GFP (P, Q) secreted from the cell in *sand-1* (O, Q). Cell boundaries in (A)–(E) are shown with the dotted lines. The values of Pearson (r_p) and Spearman (r_s) correlation coefficients represent the extent of colocalization between the two proteins. The values range between +1, indicating a positive correlation, and −1 for a negative correlation. Scale bars represent 1 cm (H, I); 100 μm (J); 5 μm (K–M); 20 μm (N–Q). See also Figures S1 and S2.

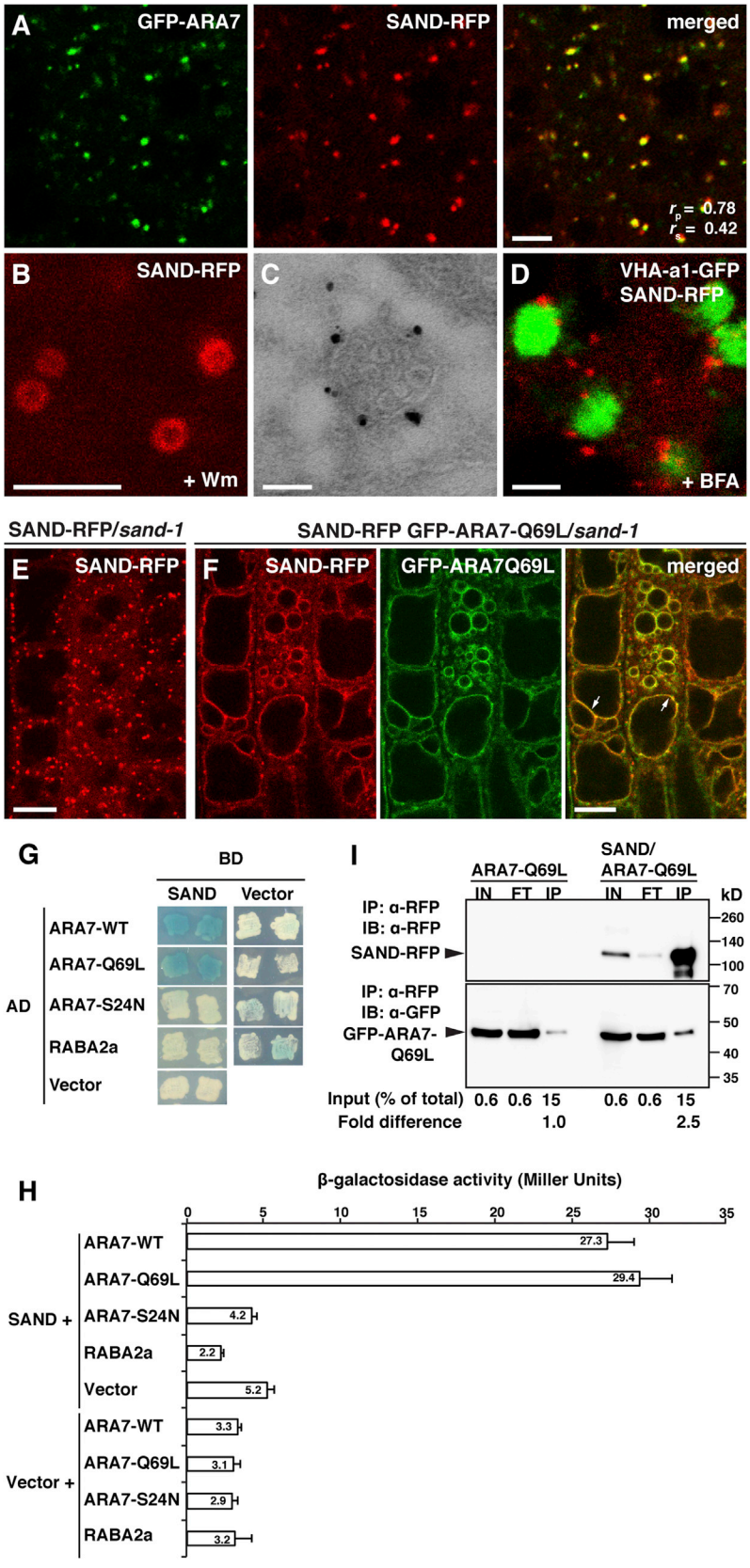

Figure 3. SAND Protein Localization and Interaction with Rab5-like ARA7

(A) Colocalization of SAND-RFP with GFP-ARA7. The values of Pearson (r_p) and Spearman (r_s) correlation coefficients represent the extent of colocalization between the two proteins. The values range between +1, indicating a positive correlation, and −1 for a negative correlation. See also Figure S3A.

(B) Enlarged ring-shaped signals of SAND-RFP in response to wortmannin treatment.

(C) Immuno-gold localization of SAND-RFP on limiting membrane of MVB.

(D) Double-labeling of TGN-localized VHA-a1-GFP and SAND-RFP in BFA-treated root cells. Note the close association of SAND signal (red) with VHA-a1-positive BFA compartment (green).

(E) SAND localization in rescued *sand-1* mutant.

(F) Double labeling of GFP-ARA7-Q69L (GTP-locked form) and SAND in rescued *sand-1* mutant. Note the colocalization of the two proteins in the vacuolar membrane (arrows).

(G) Yeast two-hybrid interaction analysis of SAND with ARA7 wild-type (WT), GTP-locked (Q69L), GDP-locked (S24N) forms, and RABA2a (TGN-localized; contr).

(H) Quantitation of SAND-ARA7 interaction strength in yeast, using β-galactosidase activity. Data shown as means ± SE; n = 5.

(I) Coimmunoprecipitation of ARA7-Q69L with SAND. *Arabidopsis* seedlings stably expressing both SAND-RFP and GFP-ARA7-Q69L, in *sand-1* background, were used for precipitation with anti-RFP antibody-linked agarose beads. Seedlings expressing only GFP-ARA7-Q69L were used as control. Upper half of the membrane was detected with anti-RFP antibody whereas lower half was used for anti-GFP antibody detection. The signal intensity of GFP-ARA7-QL band in IP relative to their respective inputs was used to calculate fold change. IN, input; FL, flow-through; IP, immunoprecipitate; IB, immunoblot; kD, kilodalton. Input (%) represents loading volume relative to the total volume used for IP.

Scale bars represent 5 μm (A, B, D); 100 nm (C); 10 μm (E, F). See also Figures S3 and S4.

TGN-localized VHA-a1 was largely unaffected. However, the vacuolar membrane was faintly labeled in *sand-1*, in addition to the exclusive labeling of the TGN in wild-type (Figures 2A and 2B). In contrast, two Rab5-like GTPases, ARA6 (aka RABF1) [22] and ARA7 (aka RABF2b), labeled clusters of abnormally shaped endosomal structures, which ultrastructural analysis identified as clusters of enlarged MVBs containing intraluminal vesicles (Figures 2C–2H). The mutant MVBs were approximately 60% larger than wild-type MVBs in diameter and had slightly fewer intraluminal vesicles (Figures 2G, 2H, and S2I). Interestingly, ARA6 (RABF1) and YFP-2xFYVE labeled the vacuolar membrane in *sand-1* mutants (Figures 2E, 2F, S2G, and S2H, arrowhead). Thus, SAND appears to act at the MVB.

SAND colocalized with ARA7 (RABF2b) and, like ARA7, was responsive to the PI3-kinase inhibitor wortmannin [23], yielding ring-shaped signals (Figures 3A, 3B, and S3A). Consistent with these findings, SAND localized to the limiting membrane of MVBs by immunogold labeling of ultrastructural sections (Figure 3C). Furthermore, the SAND-positive compartment did not respond to BFA treatment (Figure 3D). SAND also did not colocalize with TGN-resident VHA-a1 but largely colocalized

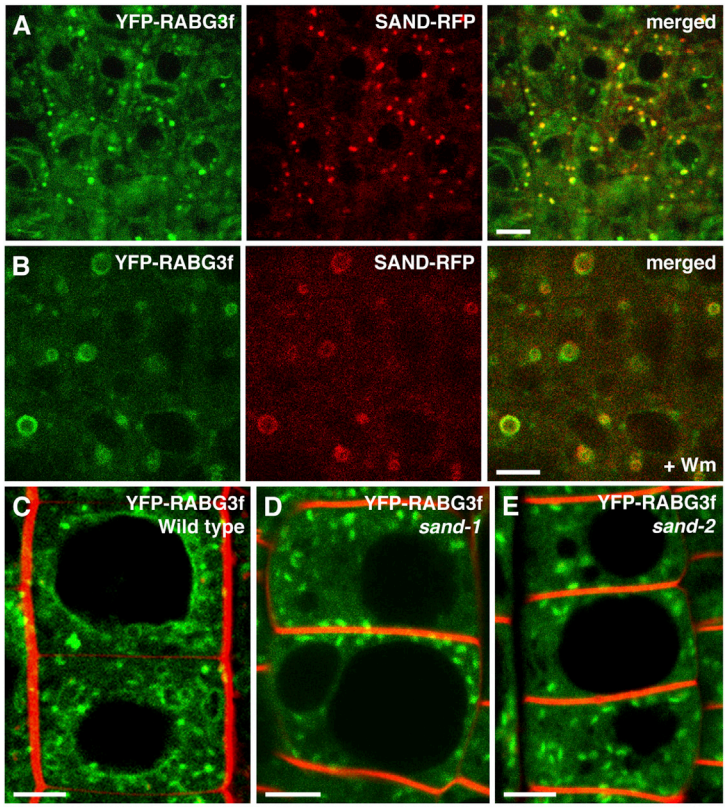

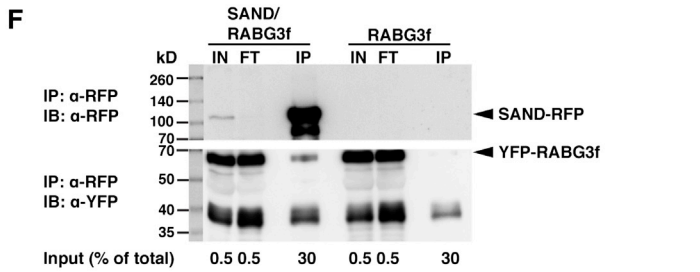

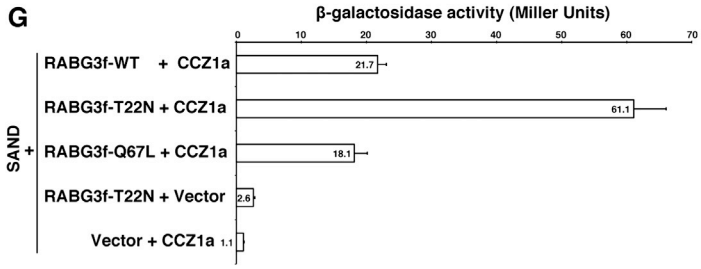

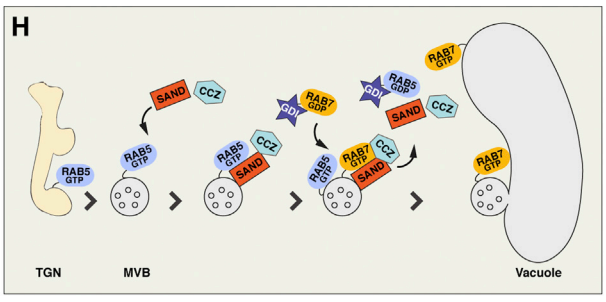

Figure 4. Role of SAND in Localization of Rab7-like RABG3f and Interaction of SAND-CCZ1 with Its GDP-Locked Isoform

(A) Colocalization of SAND-RFP and RabG3f in punctate structures.

(B) Colocalization of SAND-RFP and RabG3f in enlarged ring-shaped structures in wortmannin (Wm)-treated root cells.

(C) RabG3f localized to punctate structures and vacuolar membrane in wild-type.

(D and E) RabG3f localized to punctate structures and in the cytosol but not at the vacuolar membrane in *sand-1* (D) and *sand-2* (E).

(F) Coimmunoprecipitation of RABG3f with SAND. Immunoprecipitation was performed with transgenic line expressing both SAND-RFP and YFP-RABG3f and anti-RFP antibody-linked agarose beads. Seedlings expressing only YFP-RABG3f were used as control. Upper part of the membrane was developed with anti-RFP antibody and lower part was visualized with anti-YFP antibody. IN, input; FL, flow-through; IP, immunoprecipitate; IB, immunoblot; kD, kilodalton. Input (%) represents loading volume relative to the total volume used for IP.

(G) Quantitation of interaction strength between SAND (fused to binding domain) and wild-type (WT), GTP-locked (Q67L), or GDP-locked (T22N) isoforms of RABG3f (fused to activation domain) in presence or absence of CCZ1 protein in yeast three-hybrid assay using β-galactosidase reporter activity. Data shown as means ± SE; n = 5.

(H) Model of SAND protein action in vacuolar trafficking. RAB5 (ARA7) is recruited at the TGN and remains bound to the limiting membrane of newly formed MVB where it recruits SAND protein. Once present on MVB, SAND together with CCZ1 protein leads to the activation of RAB7 (RABG3f) on MVB and its fusion with vacuole.

Scale bars represent 5 μm (A–E). See also Figure S4.

with the PI3P sensor 2xFYVE and Rab5-like ARA6 (Figure S3). Constitutive activity of ARA7-Q69L [24, 25] (GTP-locked form) resulted in its vacuolar membrane localization (Figure 3F). Interestingly, in the presence of constitutively active ARA7, SAND was also detected on the enlarged MVBs and at the vacuolar membrane (Figures 3E and 3F). To examine whether SAND interacts with ARA7 directly, yeast two-hybrid interaction assays were performed. Both the wild-type form of ARA7 and the GTP-locked form (ARA-Q69L) interacted with SAND whereas the GDP-locked form (ARA7-S24N) did not (Figures 3G, 3H, S4A, and S4B). Interaction of SAND-RFP with GFP-tagged ARA7-Q69L was also detected by coimmunoprecipitation in extracts of transgenic *Arabidopsis* seedlings (Figure 3I). Thus, SAND appears to be an effector of GTP-bound ARA7.

In yeast, SAND/Mon1 forms a heterodimer with CCZ1 that acts as a guanine-nucleotide exchange factor (GEF) of late-endosomal/vacuolar Rab7-like Ypt7 [8]. In *Arabidopsis*, there are eight Rab7-like GTPases including RABG3f, which has been localized to MVBs and the vacuole [26, 27]. RABG3f colocalized with SAND protein both in untreated and in wortmannin-treated seedling roots, displaying ring-shaped signals upon wortmannin treatment (Figures 4A and 4B). Furthermore, YFP-tagged RABG3f localized to MVBs and the vacuolar membrane in wild-type roots (Figure 4C). In contrast, no YFP signal was detected on the vacuolar membrane in *sand-1* mutant seedling roots. Instead, RABG3f was present in punctae and in the cytosol (Figures 4D, 4E, and S4E). These punctate structures did not respond to wortmannin in *sand-1*, in contrast to wild-type, suggesting that they are not MVBs (Figure S4E). Thus, SAND is required for the correct localization of

RABG3f including its accumulation on the vacuolar membrane, which is similar to the dependence of Rab7-like Ypt7 on Mon1/SAND in yeast [28]. These data suggested that SAND, directly or indirectly, might interact with RABG3f. Indeed, interaction was detected in coimmunoprecipitation assays via extracts of transgenic plants that expressed SAND-RFP and YFP-tagged RABG3f (Figure 4F). We then employed yeast three-hybrid analysis involving CCZ1 as a bridging protein to characterize the potential interaction between SAND and RABG3f (Figures 4G, S4A, S4C, and S4D). In the presence of CCZ1, SAND interacted much more strongly with the GDP-locked form of RABG3f than with wild-type or the GTP-locked form, which would be consistent with a role for SAND-CCZ1 as RABG3f-GEF (see also the accompanying manuscript by Ebine et al [29]., which demonstrates RabG3f-GEF activity of SAND-CCZ1). Moreover, SAND alone did not interact with the GDP-locked form of RABG3f, suggesting that the coimmunoprecipitation of RABG3f with SAND from plant extracts actually involved the presence of the SAND-CCZ1 heterodimer.

Our results indicate that in plants, as has been described in nonplant organisms, protein trafficking to the vacuole for degradation involves endosomal maturation from early endosome to MVB and subsequent fusion of MVBs with the vacuole (see model in Figure 4H). In addition, the role of SAND protein in Rab5-to-Rab7 conversion appears to be evolutionarily conserved. Surprisingly, however, SAND-mediated Rab conversion is not required for MVB formation in *Arabidopsis*, as revealed by the presence of intraluminal vesicles in *sand* mutant plants, indicating that maturation of late endosomes from early endosomes takes place in the presence of Rab5 and the absence of Rab7. Instead, in plants Rab conversion by SAND is specifically required for the subsequent MVB-vacuole fusion. It is conceivable, though, that SAND-mediated Rab conversion might also play a role in MVB-vacuole/lysosome fusion in nonplant organisms, as suggested by the interaction of Rab7-like Ypt7 with the vacuolar HOPS complex [8]. However, this might not be readily apparent because of the earlier requirement of SAND protein in endosomal maturation such that functional MVBs are not generated in *sand* mutants. The underlying difference between plants and nonplant organisms thus relates to a difference in specific membrane recruitment and/or activation of Rab5-like GTPases, with ARA6 and ARA7 of *Arabidopsis* mainly associating with MVBs/LEs and Rab5 and yeast Vps21p associating with early endosomes [30]. It is tempting to speculate that the difference between plants and nonplant organisms observed in endosomal maturation and Rab conversion might result from the relative timing of two distinct processes: ESCRT-dependent formation of intraluminal vesicles, which transforms early into late endosomes, and Rab5-to-Rab7 conversion, which essentially prepares late endosomes/MVBs for their fusion with the lysosome/vacuole.

Supplemental Information

Supplemental Information includes four figures and Supplemental Experimental Procedures and can be found with this article online at http://dx.doi.org/10.1016/j.cub.2014.05.005.

Acknowledgments

We thank Niko Geldner, Ueli Grossniklaus, and Takashi Ueda for sharing published materials and Sacco de Vries for kindly providing anti-YFP antiserum and NASC for T-DNA insertion lines. This work was funded by DFG grant Ju179/18-1.

Received: February 12, 2014
Revised: April 7, 2014
Accepted: May 2, 2014
Published: May 29, 2014

References

1. Huotari, J., and Helenius, A. (2011). Endosome maturation. EMBO J. *30*, 3481–3500.
2. Henne, W.M., Buchkovich, N.J., and Emr, S.D. (2011). The ESCRT pathway. Dev. Cell *21*, 77–91.
3. Poteryaev, D., Datta, S., Ackema, K., Zerial, M., and Spang, A. (2010). Identification of the switch in early-to-late endosome transition. Cell *141*, 497–508.
4. Otegui, M.S., and Spitzer, C. (2008). Endosomal functions in plants. Traffic *9*, 1589–1598.
5. Richter, S., Voss, U., and Jürgens, G. (2009). Post-Golgi traffic in plants. Traffic *10*, 819–828.
6. Reyes, F.C., Buono, R., and Otegui, M.S. (2011). Plant endosomal trafficking pathways. Curr. Opin. Plant Biol. *14*, 666–673.
7. Rink, J., Ghigo, E., Kalaidzidis, Y., and Zerial, M. (2005). Rab conversion as a mechanism of progression from early to late endosomes. Cell *122*, 735–749.
8. Nordmann, M., Cabrera, M., Perz, A., Bröcker, C., Ostrowicz, C., Engelbrecht-Vandré, S., and Ungermann, C. (2010). The Mon1-Ccz1 complex is the GEF of the late endosomal Rab7 homolog Ypt7. Curr. Biol. *20*, 1654–1659.
9. Kinchen, J.M., and Ravichandran, K.S. (2010). Identification of two evolutionarily conserved genes regulating processing of engulfed apoptotic cells. Nature *464*, 778–782.
10. Dettmer, J., Hong-Hermesdorf, A., Stierhof, Y.D., and Schumacher, K. (2006). Vacuolar H+-ATPase activity is required for endocytic and secretory trafficking in *Arabidopsis*. Plant Cell *18*, 715–730.
11. Contento, A.L., and Bassham, D.C. (2012). Structure and function of endosomes in plant cells. J. Cell Sci. *125*, 3511–3518.
12. Viotti, C., Bubeck, J., Stierhof, Y.D., Krebs, M., Langhans, M., van den Berg, W., van Dongen, W., Richter, S., Geldner, N., Takano, J., et al. (2010). Endocytic and secretory traffic in *Arabidopsis* merge in the trans-Golgi network/early endosome, an independent and highly dynamic organelle. Plant Cell *22*, 1344–1357.
13. Stierhof, Y.D., and El Kasmi, F. (2010). Strategies to improve the antigenicity, ultrastructure preservation and visibility of trafficking compartments in *Arabidopsis* tissue. Eur. J. Cell Biol. *89*, 285–297.
14. Vermeer, J.E., van Leeuwen, W., Tobeña-Santamaria, R., Laxalt, A.M., Jones, D.R., Divecha, N., Gadella, T.W., Jr., and Munnik, T. (2006). Visualization of PtdIns3P dynamics in living plant cells. Plant J. *47*, 687–700.
15. Scheuring, D., Viotti, C., Krüger, F., Künzl, F., Sturm, S., Bubeck, J., Hillmer, S., Frigerio, L., Robinson, D.G., Pimpl, P., and Schumacher, K. (2011). Multivesicular bodies mature from the trans-Golgi network/early endosome in *Arabidopsis*. Plant Cell *23*, 3463–3481.
16. Robinson, D.G., Jiang, L., and Schumacher, K. (2008). The endosomal system of plants: charting new and familiar territories. Plant Physiol. *147*, 1482–1492.
17. Fuji, K., Shimada, T., Takahashi, H., Tamura, K., Koumoto, Y., Utsumi, S., Nishizawa, K., Maruyama, N., and Hara-Nishimura, I. (2007). *Arabidopsis* vacuolar sorting mutants (green fluorescent seed) can be identified efficiently by secretion of vacuole-targeted green fluorescent protein in their seeds. Plant Cell *19*, 597–609.
18. Sohn, E.J., Kim, E.S., Zhao, M., Kim, S.J., Kim, H., Kim, Y.W., Lee, Y.J., Hillmer, S., Sohn, U., Jiang, L., and Hwang, I. (2003). Rha1, an *Arabidopsis* Rab5 homolog, plays a critical role in the vacuolar trafficking of soluble cargo proteins. Plant Cell *15*, 1057–1070.
19. Reichardt, I., Stierhof, Y.D., Mayer, U., Richter, S., Schwarz, H., Schumacher, K., and Jürgens, G. (2007). Plant cytokinesis requires de novo secretory trafficking but not endocytosis. Curr. Biol. *17*, 2047–2053.
20. Geldner, N., Friml, J., Stierhof, Y.D., Jürgens, G., and Palme, K. (2001). Auxin transport inhibitors block PIN1 cycling and vesicle trafficking. Nature *413*, 425–428.

21. Abas, L., Benjamins, R., Malenica, N., Paciorek, T., Wiśniewska, J., Moulinier-Anzola, J.C., Sieberer, T., Friml, J., and Luschnig, C. (2006). Intracellular trafficking and proteolysis of the *Arabidopsis* auxin-efflux facilitator PIN2 are involved in root gravitropism. Nat. Cell Biol. *8*, 249–256.
22. Ebine, K., Fujimoto, M., Okatani, Y., Nishiyama, T., Goh, T., Ito, E., Dainobu, T., Nishitani, A., Uemura, T., Sato, M.H., et al. (2011). A membrane trafficking pathway regulated by the plant-specific RAB GTPase ARA6. Nat. Cell Biol. *13*, 853–859.
23. Takáč, T., Pechan, T., Samajová, O., Ovečka, M., Richter, H., Eck, C., Niehaus, K., and Samaj, J. (2012). Wortmannin treatment induces changes in *Arabidopsis* root proteome and post-Golgi compartments. J. Proteome Res. *11*, 3127–3142.
24. Ueda, T., Yamaguchi, M., Uchimiya, H., and Nakano, A. (2001). Ara6, a plant-unique novel type Rab GTPase, functions in the endocytic pathway of *Arabidopsis thaliana*. EMBO J. *20*, 4730–4741.
25. Jia, T., Gao, C., Cui, Y., Wang, J., Ding, Y., Cai, Y., Ueda, T., Nakano, A., and Jiang, L. (2013). ARA7(Q69L) expression in transgenic *Arabidopsis* cells induces the formation of enlarged multivesicular bodies. J. Exp. Bot. *64*, 2817–2829.
26. Rutherford, S., and Moore, I. (2002). The *Arabidopsis* Rab GTPase family: another enigma variation. Curr. Opin. Plant Biol. *5*, 518–528.
27. Geldner, N., Dénervaud-Tendon, V., Hyman, D.L., Mayer, U., Stierhof, Y.D., and Chory, J. (2009). Rapid, combinatorial analysis of membrane compartments in intact plants with a multicolor marker set. Plant J. *59*, 169–178.
28. Cabrera, M., and Ungermann, C. (2013). Guanine nucleotide exchange factors (GEFs) have a critical but not exclusive role in organelle localization of Rab GTPases. J. Biol. Chem. *288*, 28704–28712.
29. Ebine, K., Inoue, T., Ito, J., Ito, E., Uemura, T., Goh, T., Abe, H., Sato, K., Nakano, A., and Ueda, T. (2014). Plant vacuolar trafficking occurs through distinctly regulated pathways. Curr. Biol. *24*, this issue.
30. Markgraf, D.F., Peplowska, K., and Ungermann, C. (2007). Rab cascades and tethering factors in the endomembrane system. FEBS Lett. *581*, 2125–2130.

Note Added in Proof

An independent analysis of MON1, which is allelic to SAND, was recently reported (Cui et al., *The Plant Cell*, in press). Although Cui and colleagues used a different mutant allele and different trafficking markers, their study yielded essentially the same conclusion.